JACS
JOURNAL OF THE AMERICAN CHEMICAL SOCIETY
Article
pubs.acs.org/JACS

Direct Spectroscopic Detection and EPR Investigation of a Ground State Triplet Phenyl Oxenium Ion

Ming-De Li,[†] Toshia R. Albright,[‡] Patrick J. Hanway,[‡] Mingyue Liu,[†] Xin Lan,[†] Songbo Li,[†] Julie Peterson,[‡] Arthur H. Winter,*[,‡] and David Lee Phillips*[,†]

[†]Department of Chemistry, University of Hong Kong, Pokfulam Road, Hong Kong, S.A.R., P. R. China
[‡]Department of Chemistry, Iowa State University, 2101d Hach Hall, Ames, Iowa 50011, United States

Supporting Information

ABSTRACT: Oxenium ions are important reactive intermediates in synthetic chemistry and enzymology, but little is known of the reactivity, lifetimes, spectroscopic signatures, and electronic configurations of these unstable species. Recent advances have allowed these short-lived ions to be directly detected in solution from laser flash photolysis of suitable photochemical precursors, but all of the studies to date have focused on aryloxenium ions having closed-shell singlet ground state configurations. To study alternative spin configurations, we synthesized a photoprecursor to the *m*-dimethylamino phenyloxenium ion, which is predicted by both density functional theory and MRMP2 computations to have a triplet ground state electronic configuration. A combination of femtosecond and nanosecond transient absorption spectroscopy, nanosecond time-resolved Resonance Raman spectroscopy (ns-TR^3), cryogenic matrix EPR spectroscopy, computational analysis, and photoproduct studies allowed us to trace essentially the complete arc of the photophysics and photochemistry of this photoprecursor and permitted a first look at a triplet oxenium ion. Ultraviolet photoexcitation of this precursor populates higher singlet excited states, which after internal conversion to S_1 over 800 fs are followed by bond heterolysis in ~1 ps, generating a hot closed-shell singlet oxenium ion that undergoes vibrational cooling in ~50 ps followed by intersystem crossing in ~300 ps to generate the triplet ground state oxenium ion. In contrast to the rapid trapping of singlet phenyloxenium ions by nucleophiles seen in prior studies, the triplet oxenium ion reacts via sequential H atom abstractions on the microsecond time domain to ultimately yield the reduced *m*-dimethylaminophenol as the only detectable stable photoproduct. Band assignments were made by comparisons to computed spectra of candidate intermediates and comparisons to related known species. The triplet oxenium ion was also detected in the ns-TR^3 experiments, permitting a more clear assignment and identifying the triplet state as the π,π^* triplet configuration. The triplet ground state of this ion was further supported by photolysis of the photoprecursor in an ethanol glass at ~4 K and observing a triplet species by cryogenic EPR spectroscopy.

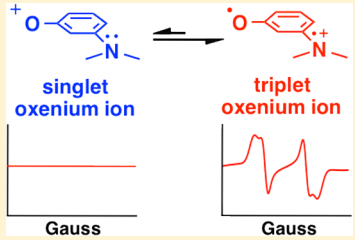

INTRODUCTION

Oxenium ions are reactive intermediates of formula R−O$^+$. These species are the isoelectronic oxygen analogue of the more familiar nitrene class of intermediates, but bear a formal positive charge on a hypovalent oxygen. Like nitrenes, oxenium ions can be stabilized by transition metals,[1] acting as novel ligands, but in their free form they are short-lived in solution, as might be expected of a species forced to suffer from such an inharmonious electronic arrangement. Of more synthetic relevance, these transient species have often been proposed as intermediates in a number of synthetically useful oxidation reactions of phenols,[2−6] including the oxidative Hosomi−Sakurai reaction[7,8] and Wagner−Meerwin transposition,[9] electrochemical oxidations of phenols and phenolates,[10,11] and a plethora of other phenolic oxidations and tautomerization reactions. They are also suggested to be key intermediates in the industrial production of materials like poly(phenyl)ether (PPE), an industrial thermoplastic.[12−14] In addition, the enzymatic oxidative mechanisms of phenols to quinones are proposed to involve the intermediacy of discrete oxenium ions,[15] Despite their chemical importance, mechanistic studies of oxenium ions are limited.

Previous experimental studies of aryloxenium ions have been performed by either photochemical or thermal generation methods. In the 1970s and early 1980s, Abramovitch and Okamoto used thermolytic methods to generate aryloxenium ions. Studies of their stable end products permitted indirect characterizations of their reactivity.[13,14] Later, Novak and co-workers investigated the reactivities of aryloxenium ions using both thermal and photochemical generation methods.[16] Only recently have aryloxenium ions been directly detected by laser flash photolysis in solution. In 2007, Novak, Platz, and co-workers reported the first direct detection of an aryloxenium ion in solution (a biphenylyl oxenium ion) using laser flash photolysis, providing definitive evidence that these reactive ions are in fact discrete intermediates in solution.[17]

Like nitrenes, oxenium ions can adopt different electronic configurations. The electronic state energies of phenyl oxenium

Received: June 17, 2015
Published: July 22, 2015

DOI: 10.1021/jacs.5b06302
J. Am. Chem. Soc. 2015, 137, 10391−10398

ions and some simple substituted derivatives have previously been computed using the CASPT2//CASSCF computational method.[18−20] These computational studies suggested that oxenium ions undergo large changes in the electronic state orderings by changing the substituent attached to the formally positive oxygen. For instance, the simplest oxenium ion, OH^+, has degenerate frontier orbitals and a triplet ground state with a gap of 54 kcal/mol to the lowest energy singlet state.[21] Substituting the hydrogen with a phenyl ring leads to the lowest-energy state being a closed-shell singlet ground state by ∼20 kcal/mol. Computations suggest most simple aryloxenium ions are closed-shell singlet ground state species,[19] although heteroaryl oxenium ions may adopt alternative electronic states.[20] The singlet ground state of the phenyl oxenium ion is supported by both photoelectron spectroscopy[22] and the results from these high-level computational methods.

Following Novak and Platz's detection of a substituted biphenylyl oxenium ion derivative, we used selected protonated hydroxylamine salts as novel photoprecursors to generate both the parent phenyloxenium ion and the biphenylyl oxenium ion as a product from the photoheterolysis of the aryl hydroxylamine tetrafluoroborate salt.[23] In addition to a concomitant homolytic process, these hydroxylamine salts also undergo heterolytic scission of the O−N bond to lead to the generation of the singlet aryloxenium ion and neutral ammonia.[23,24] These results allowed comparisons to the neutral photoprecursor studied by Novak, Platz, and co-workers,[25] highlighting the unique differences in the photochemistry/photophysics of the precursors.[26] To summarize the prior results, the aryloxenium ions studied thus far have had closed-shell singlet ground states and lifetimes of a few nanoseconds in solution, typically reacting with nucleophiles (e.g., ammonia, chloride, water) at the *ortho* and *para* positions to generate ring-substituted phenols as the ultimate stable photoproducts. See Figure 1. To date, essentially nothing is known about the reactivity of triplet aryloxenium ions.

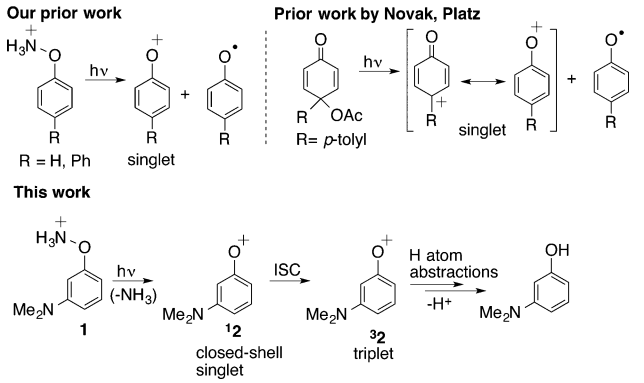

Figure 1. Overview of this work and prior work.

Computational studies have suggested that simple ring substituents could lead to significant changes in the singlet−triplet energy gap (ΔE_{ST}).[19] A recent computational study on the effect of *meta* substitution on the ΔE_{ST} of phenyloxenium ions found that substituting the *meta* positions of the phenyloxenium ions with pi donors (e.g., NH_2) stabilizes an *m*-xylylene-like π,π^* triplet state in preference to the singlet state.[18] For the *m*-amino phenyloxenium ion, the ground state was computed to be the triplet state by DFT computations, but was computed to have essentially degenerate singlet and triplet energies at the CASPT2/pVTZ level of theory. Consequently, the ground state of the *m*-amino phenyloxenium ion cannot be predicted with certainty. Although not explicitly considered in that study, our thought was that the *m*-dimethylamino phenyloxenium, bearing a stronger *meta* π donor than an amino substituent, might have a more definitively triplet ground state.

All of the prior studies that directly detected aryloxenium ions studied oxenium ions that had closed-shell singlet ground states. We were interested in detecting a triplet ground state oxenium ion in order to understand the spin-selective reactivity of oxenium ions and to be able to compare the lifetimes, properties, and reaction types of triplet oxenium ions to their closed-shell singlet counterparts. Thus, we synthesized the *m*-dimethylamino phenylhydroxylamine (*m*-DMAP) salt **1**, which we anticipated could generate a ground state triplet aryloxenium ion ^{3}**2** upon photolysis. The different electronic configurations possible for the aryloxenium ion are depicted in Figure 2.

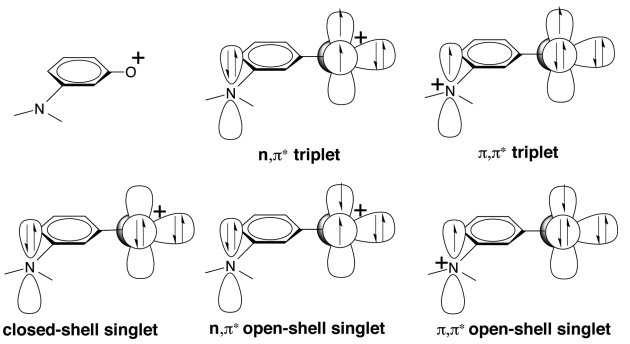

Figure 2. Possible schematic electronic configurations considered for the *m*-dimethylamino phenyloxenium ion **2**. Computations suggest the ground configuration is the π,π^* triplet configuration and the lowest energy singlet state is the closed-shell configuration.

Here, we report a combined femtosecond transient absorbance (fs-TA), nanosecond transient absorbance (ns-TA), and nanosecond time-resolved resonance Raman (ns-TR^3) spectroscopic investigation of the photophysics and photochemistry of *m*-DMAP **1** that allowed us to directly observe the formation of the ground state triplet phenyloxenium ion after ultraviolet photoexcitation in a MeCN/H_2O solution. We also studied the triplet ion by cryogenic matrix photolysis of the photoprecursor in an EtOH glass and observed a triplet species in the electron paramagnetic resonance (EPR) spectrum at 4 K, providing strong evidence for this ion having a triplet ground state. To our knowledge this is the first direct observation and reactivity study of a ground state triplet oxenium ion in solution using LFP, and the first EPR detection of a triplet aryloxenium ion.

EXPERIMENTAL AND COMPUTATIONAL METHODS

The *m*-dimethylamino phenylhydroxylamine **1** photoprecursor was synthesized, purified, and characterized via standard methods (see the Supporting Information for synthetic procedures and spectra). Spectroscopic grade acetonitrile (MeCN) and deionized water were used to prepare the sample solutions for use in the time-resolved spectroscopy experiments. In all of the time-resolved experiments, the sample solutions were purged with argon for 30 min. During the experiments, the sample solutions were also purged with argon.

DOI: 10.1021/jacs.5b06302
J. Am. Chem. Soc. 2015, 137, 10391−10398

1. Femtosecond Transient Absorption (fs-TA) Experiments. The fs-TA experiments were performed by employing an experimental setup and methods detailed previously.[27] Only a brief description is provided here. Fs-TA measurements were accomplished using a femtosecond regenerative amplified Ti:sapphire laser system in which the amplifier was seeded with the 120 fs laser pulses from an oscillator laser system. The laser probe pulse was produced by utilizing ∼5% of the amplified 800 nm laser pulses to generate a white-light continuum (340−700 nm) in a CaF_2 crystal and then this probe beam was split into two parts before traversing the sample. One probe laser beam goes through the sample while the other probe laser beam goes to the reference spectrometer in order to monitor the fluctuations in the probe beam intensity. For the experiments discussed in this work, a 40 mL solution was flowed through a 2 mm path length cuvette to avoid problems with interference from photolysis of secondary photoproducts. This flowing sample was excited by a 267 nm pump laser beam. An absorbance of **1** at 267 nm was used for the sample solutions for the fs-TA experiments in order to maintain the same number of photons being absorbed for the same irradiating conditions for the samples.

2. Nanosecond Transient Absorption (ns-TA) Experiment. The ns-TA experiments were performed using a commercial laser flash photolysis apparatus. The fourth harmonic output of an Nd:YAG laser supplied the 266 nm laser pump pulse. The probe light came from a 450 W xenon lamp. The 266 nm pump laser beam photoexcited the sample, and at a right angle the probe light from the xenon lamp traversed the sample held in a 1 cm flowing quartz cell. The transmitted probe light was then detected by a single detector (for kinetic analysis) or by an array detector (for spectral analysis). The changes in the light transmission signals were normally converted into changes of optical density (ΔOD) and these signals were then analyzed by a monochromator equipped with a photomultiplier to detect the light. Unless specified otherwise, the ns-TA experiments were performed in argon purged solutions and the sample solutions were made up to have an absorbance of 1 at 266 nm.

3. Nanosecond Time-Resolved Resonance Raman (ns-TR^3) Experiments. The ns-TR^3 experiments were performed employing an experimental setup and methods detailed previously and only a brief account is provided here.[28] The fourth harmonic of a Nd:YAG nanosecond pulsed laser supplied the 266 nm pump wavelength and the 355 nm probe wavelength came from the third harmonic of a second Nd:YAG laser. The pump pulse photoexcited the sample to start the photochemical processes and the probe pulse monitored the sample and the intermediate species formed. The laser beams were lightly focused and lined up so that they merged together onto a flowing argon purged sample solution. A pulse delay generator was utilized to electronically set the time delay between the pump and probe laser pulses. The Raman scattered signal was collected using a backscattering geometry and observed by a liquid nitrogen-cooled charge-coupled device (CCD) detector. The ns-TR^3 spectra shown here were found from subtraction of an appropriately scaled probe-before-pump spectrum from the correlated pump−probe resonance Raman spectrum to mostly get rid of nontransient bands. The Raman bands of MeCN were used to calibrate the Raman shifts with an estimated uncertainty of 5 cm^{-1}.

4. Product and Matrix isolation EPR Studies. Photolysis studies were performed as follows: addition of 10 mg of *m*-dimethylaminophenylhydroxylamine hydrochloride **1** and 5−10 mg of sodium acetate trihydrate (internal standard) were added to 0.8 mL of deuterium oxide and placed in a quartz NMR tube. An initial ^{1}H NMR was taken with a 90° angle and a relaxation delay of 60 s. The solution was then degassed for 30 min (under argon) and photolyzed for 1 h in a Rayonet photoreactor fitted with 254 nm bulbs. At different time intervals of photolysis, NMR spectra were taken with the previous parameters. At 44% conversion of starting material, 89% mass balance of 3-dimethylaminophenol was observed. No other products were seen by ^{1}H NMR (see the Supporting Information for spectra changes upon photolysis) and the remaining mass balance could be accounted for by formation of an insoluble colored tar.

Matrix EPR studies were performed using an X-band EPR spectrometer with a temperature control unit capable of achieving near liquid helium temperatures (∼4 K) and equipped with a UV-emitting mercury light source channeled into the cavity using a fiber optic cable. More detailed information on the EPR settings and EPR simulation parameters can be found in the Supporting Information.

5. Computational Studies. We computed the singlet−triplet gap (ΔE_{ST}) of the *m*-dimethylamino phenyloxenium ion **2** using density functional theory (B3LYP/6-31G(d,p)). The ΔE_{ST} at the DFT level of theory was computed to be +12.5 kcal/mol in favor of the triplet state. Because we found a RHF → UHF instability in the singlet state by DFT, for added confidence an MRMP2(8,8)/6-31G(d)//MCSCF-(8,8)/6-31G(d) calculation was also performed using a complete π active space. At this level of theory, the ΔE_{ST} is computed to be +9.3 kcal/mol in favor of the triplet state and the lowest energy singlet state is found to be the closed shell configuration. Thus, the computational studies make a clear prediction that the triplet state is the lowest energy electronic configuration for **2**, with the triplet state being a π,π^* configuration. This π,π^* triplet configuration can be arrived at conceptually by starting with the closed-shell singlet state and transferring an electron from the nitrogen lone pair to the empty π^* orbital associated with oxenium ion center. See Figure 2. The TD-DFT methodology was performed to predict the UV−vis absorption spectra of the candidate transient species generated from the photolysis of the photoprecursor (TD-B3LYP/6-311G(2d,p)).[29] GaussSum software was utilized to simulate the UV−vis spectra.[30] To predict the TR^3 spectra, second-order Møller−Plesset perturbation theory (MP2) with a 6-311G(d,p) basis set was employed to optimize the structures and predict the Raman spectra of key intermediates. A Lorentzian function with a 15 cm^{-1} bandwidth for the vibrational frequencies and a frequency scaling factor of 0.974 was used in the comparison of the calculated results with the experimental spectra.[31] No imaginary frequency modes were observed at the stationary states of the optimized structures. All of the calculations were done using the Gaussian 03/09 program[32] except for the MRMP2//MCSCF computations, which were computed with the GAMESS software.[33]

RESULTS AND DISCUSSION

1. Femtosecond Transient Absorption Investigation of *m*-Dimethylamino Phenylhydroxylamine Hydrochloride 1. Figure 3 shows the evolution of the transient absorption

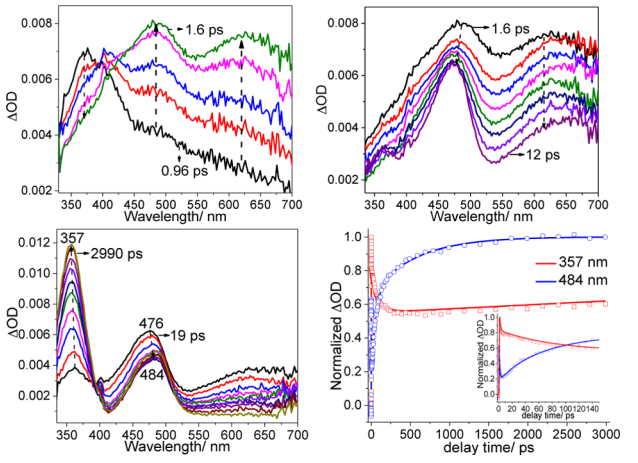

Figure 3. Shown are the fs-TA spectra of species produced in a MeCN/H_2O 1:1 solution acquired after 266 nm irradiation of the precursor *m*-DMAP. (Top left) LFP from 0.96 to 1.6 ps; (top right) from 1.6 to 12 ps; (bottom left) from 19 to 2990 ps. Bottom right shows the kinetics of the characteristic fs-TA absorption bands observed at 357 and 484 nm for the fs-TA spectra observed after 266 nm photoexcitation of *m*-DMAP **1** in a MeCN/H_2O 1:1 solution. See the text for more details.

DOI: 10.1021/jacs.5b06302
J. Am. Chem. Soc. 2015, 137, 10391−10398

of *m*-dimethylamino phenylhydroxylamine (*m*-DMAP) **1** in an acetonitrile/water (MeCN/H_2O) 1:1 mixed solution from 0.96 to 2990 ps. The spectra at early (Figure 3, top left), middle (Figure 3, top right), and later delay times (Figure 3, bottom left) are given separately to more easily discern the spectral changes that take place on different time scales. First we discuss the observations and our assignments of the transients and then we detail how we made all of the assignments. When using 267 nm as excitation wavelength, the *m*-DMAP **1** can be excited to higher singlet excited states S_n. TD-DFT computations indicate that the predominant absorption of **1** at 267 nm is the S_0-S_3 transition. See the Supporting Information. Over ~800 fs, **1** undergoes internal conversion (IC) and evolves from S_n into the S_1 excited state (see Figure 1S and Table 1S for spectra from 450 to 1000 fs). After 1 ps, the absorptions are assigned to the S_1 precursor excited state having an absorption centered at ca. 360 nm. This band rapidly decays over ~1 ps into a new transient having major absorptions at 485 and 627 nm, assigned to the closed-shell singlet oxenium ion ^{1}**2**. Similarly, prior studies of the protonated hydroxylamine photoprecursors shown in Figure 1 underwent bond cleavage in ~2 ps.[26] In the top right of Figure 3, it can be seen that the broad bands centered at 485 and 627 nm slightly decayed and noticeably shifted with time toward a shorter wavelength and a longer wavelength, respectively, over ~55 ps, ultimately yielding a sharp band at 476 nm and a broader absorption band centered at ~650 nm. This process is attributed to vibrational cooling as the hot-born oxenium ion sheds heat to solvent, a phenomenon that has also been seen in the prior work following O–N bond cleavage.

Subsequently, the two bands decay over ~550 ps to generate a new band at ~485 nm. This conversion is attributed to intersystem crossing of the singlet oxenium ion ^{1}**2** to the triplet phenyloxenium ion ^{3}**2**. Finally, this band converts to a new band over ~1 μs to a band at 494 nm, attributed to the *m*-dimethylamino phenol radical cation (see Figure 7), which slowly decays into a final product at 357 nm. An isosbestic point at 394 nm indicates a clean conversion between the latter two species.

2. TD-DFT Calculated Electronic Absorption of Candidate Intermediates after *m*-DMAP 1 Photolysis. Time-dependent density functional theory (TD-DFT) computations have been previously demonstrated to be useful in estimating the absorption bands for transient species in previous work. For example, they are frequently used for assigning absorption bands for carbenes, nitrenes and oxenium ions.[24,26,34] To help assign the transients observed in the fs-TA experiments, we have performed TD-B3LYP/6-311G(2d,p) calculations to estimate the UV–vis absorption for some likely candidate species that could be generated from the excited singlet state of *m*-DMAP **1**. TD-DFT computations were done to estimate the electronic absorption spectra of the *m*-dimethylamino phenoxy radical, the triplet *m*-dimethylamino phenyloxenium ion and the singlet *m*-dimethylamino phenyloxenium ion. The results using TD-B3LYP/6-311+G(2d,p) for these calculations are shown in Figure 4. The computed absorption spectrum for the singlet *m*-dimethylamino phenyloxenium ion gives a single band at 418 nm in the 300–600 nm region, and this does not agree with the experimental spectra at early delay time (1.6–12 ps) where there are one maximum transient absorptions at about 485 nm and a tailing broad shoulder transient absorption at 627 nm (see Figure 3). We noted that singlet carbenes have been reported to form

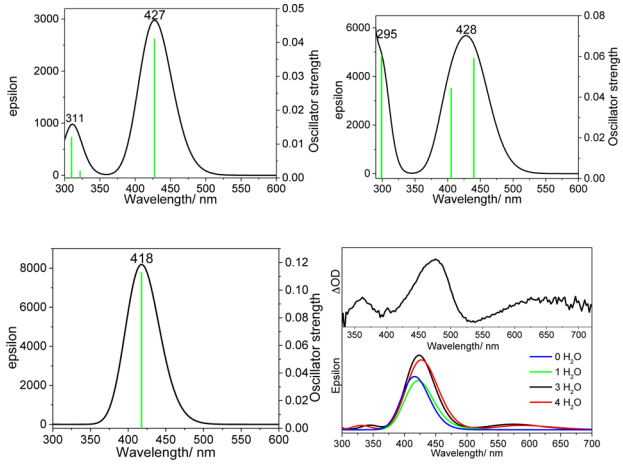

Figure 4. Shown are the computed electronic spectra of the *m*-dimethylamino phenoxy radical (top left), the triplet *m*-dimethylamino phenyloxenium ion ^{3}**2** (top right), and the singlet *m*-dimethylamino phenyloxenium ion ^{1}**2** (bottom left) from TD-B3LYP/6-311G(2d,p) calculations. Bottom right of the figure shows the experimental UV–vis spectrum at 19 ps after the pulse and the computed spectrum of the singlet *m*-dimethylamino phenyloxenium ion in the presence and absence of explicit solvent waters (note that the simulated spectrum goes to 300 nm to show smaller computed shoulder band).

complexes with solvents such as acetonitrile (and even form ylides in some cases).[35] Thus, we considered the possibility that the singlet oxenium ion was forming a solvent complex, which might alter its absorption profile. Indeed, by adding explicit complexing waters (1, 3, 4 water molecules), the computed TD-DFT absorption spectra of singlet oxenium ion in the absence of water and in the presence of one water molecule did not match with the experimental spectra at early delay time, while the simulated absorption spectra of singlet oxenium ion water adducts in the presence of 3 and 4 water molecules give reasonable agreement with the experimental bands recorded at 19 ps (see Figure 4). At much earlier times, the 476 nm band slightly shifts and decays, and the higher-wavelength 650 nm band becomes relatively smaller. TD-DFT calculation reveals that only water adducts of the singlet oxenium ion rather than the gas phase isolated singlet oxenium ion have the contribution of absorption at around 600 nm (see Figure 4). Therefore, the decay of the 650 nm band is likely associated with the vibrational cooling and the reorientation of the solvent around the singlet oxenium ion. Comparing to the isolated singlet oxenium ion, the explicitly solvated singlet oxenium ion has two new electronic transitions whose absorption bands appear at 332 and 588 nm (see Figure 4). TD-DFT calculations indicate that the electronic transition at 588 nm can be described as charge transfer in character from water to the oxenium ion while the electronic transition at 332 nm is a π,π^* transition altered by water mixing with the HOMO (see Table 2S). It is challenging to think of alternative structures to the singlet oxenium ion water complexes that would follow the singlet excited state of the photoprecursor and ultimately converts to a transient that can be assigned to the triplet oxenium ion by both UV–vis and ns-TR^3 experiments, described later; therefore, this transient is assigned to the singlet oxenium ion. Additionally, because the TD-DFT computations of the solvated closed-shell singlet oxenium ion match with the experimental bands, we assign the electronic state as the closed-shell singlet oxenium ion. This assignment is

DOI: 10.1021/jacs.5b06302
J. Am. Chem. Soc. 2015, 137, 10391–10398

consistent with the CASSCF calculations described earlier that also indicate that the lowest-energy singlet state is the closed-shell singlet state. Based on our previous study, a ground state singlet aryloxenium ion can be trapped by water molecules or other nucleophiles (chloride, ammonia). In this study, we see no trapping adducts for this oxenium ion, which might be attributed to its short lifetime, decaying into new absorption bands at 357 and 484 nm, which can still be observed at 3 ns. In addition, it should be noted that allylic strain interaction generated by the dimethylamino moiety in the *meta* position may also prevent nucleophilic additions in para and one ortho position. Although the computed absorption spectrum for the *m*-dimethylamino phenoxy radical and triplet *m*-dimethylamino phenyloxenium ion have two bands at around 300 and 428 nm, which are in good agreement with the experimental spectra in shape at later delay time (Figure 3), the observation of triplet *m*-dimethylamino phenyloxenium ion by ns-TR^3 (described later) indicates that this new transient at 357 and 484 nm should be assigned to the triplet *m*-dimethylamino phenyloxenium ion, not the *m*-dimethylamino phenoxy radical.

3. ns-TR^3 Experiments Identify the Transient at 357 nm as the π,π^* Triplet *m*-Dimethylamino Phenyloxenium Ion. In order to identify the transient species seen at around 3 ns, ns-TR^3 experiments for *m*-DMAP **1** were carried out in an aqueous acetonitrile solution. Figure 5 shows

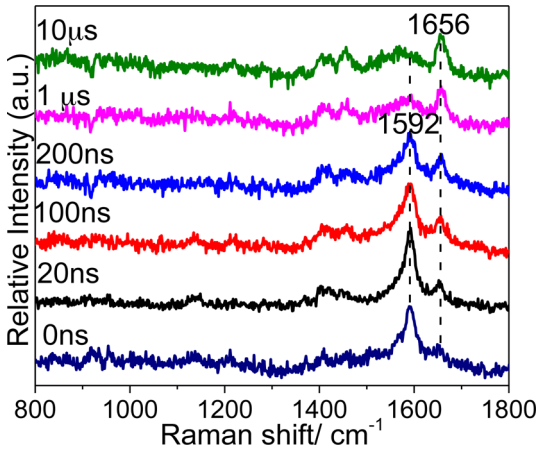

Figure 5. Shown are ns-TR^3 spectra obtained with various delay times indicated next to the spectra after 266 nm photoexcitation of *m*-dimethylamino phenyloxenium and using a 355 nm as the probe wavelength in a MeCN/H_2O 1:1 solution.

the ns-TR^3 spectra obtained with various delay times after 266 nm photoexcitation of *m*-DMAP and using 355 nm as the probe wavelength in a MeCN/H_2O 1:1 solution. The Raman band at 1592 cm^{-1} gradually drops off in intensity, which is accompanied by the growth of the Raman band at 1656 cm^{-1}. This not only indicates that there are two transient species that can be detected in the aqueous solution by the TR^3 spectra when using 355 nm as the probe wavelength, but also reveals that the first transient species with its main Raman band at 1592 cm^{-1} is the precursor of the second transient species with a main Raman band at 1656 cm^{-1}. At 10 μs, the 1592 cm^{-1} disappears, indicating that the spectrum at 10 μs arises from the second species. In an attempt to isolate the Raman spectra of the first species, the Raman spectrum obtained at 20 ns had an appropriately scaled spectrum at 10 μs subtracted from it. Figure 6 presents the ns-TR^3 spectrum obtained at 20 ns with

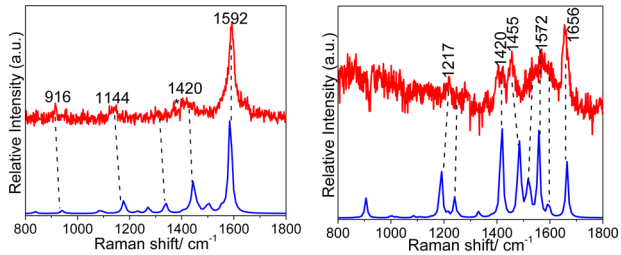

Figure 6. (Left) Comparison of the ns-TR^3 spectrum obtained at 20 ns with an appropriately scaled 10 μs spectrum subtracted from it in a MeCN/H_2O 1:1 solution (red) and the calculated normal Raman spectrum of the triplet *m*-dimethylamino phenyloxenium ion ^{3}**2** using results from MP2/6-311G(d,p) calculations (blue). (Right) Comparison of the ns-TR^3 spectrum obtained at 10 μs in a MeCN/H_2O 1:1 solution (red) and the calculated normal Raman spectrum of the *m*-dimethylamino phenol radical cation using results from B3LYP/6-311G(d,p) calculations (blue). Asterisks (*) represent solvent subtraction artifacts. See the text for more details.

the 10 μs spectrum subtracted from it in a MeCN/H_2O 1:1 solution and the calculated normal Raman spectrum of the triplet *m*-dimethylamino phenyloxenium ion **2** using results from MP2/6-311G(d,p) calculations. The experimental spectrum agrees well with the calculated normal Raman spectrum of the triplet *m*-dimethylamino phenyloxenium ion ^{3}**2** for its vibrational frequency pattern. It does not agree well with alternative candidate intermediates (^{1}**2**, or the radical). Therefore, the first species detected by the ns-TR^3 spectra in the aqueous solution can be assigned to the triplet *m*-dimethylamino phenyloxenium ion. Logically, it also seems reasonable to expect the triplet state following the singlet oxenium ion, and the computationally predicted UV−vis absorption spectrum seen in the fs-TA studies is also in reasonable agreement with the experimental value. The calculated structure of the π,π^* triplet *m*-dimethylamino phenyloxenium indicates a C−O bond length of 1.216 Å, with the electronic density delocalized into the benzene ring rather than in the C−O bond. For an aromatic ketone (e.g., such as triplet benzophenone), a C−O bond length extending up to 1.32 Å has an n,π^* triplet state character and the triplet electronic density is mainly located in the C═O group.[36−42] For the second species with a main Raman band at 1656 cm^{-1}, we tentatively assigned this species to the *m*-dimethylamino phenyloxenium radical cation which would be generated by the hydrogen abstraction of the triplet oxenium ion from the surrounding water molecules. Figure 6 (right) indicates that the computationally predicted Raman spectrum of the *m*-dimethylamino phenyloxenium radical cation is consistent with the experimental Raman spectrum obtained at 10 μs, although the noise in the spectrum at this time delay prevents a clear assignment. In the ns-TA spectra (discussed next), this transient absorbs at ~490 nm. Given that the dimethylaniline radical cation absorbs at 470 nm, it seems plausible that the *m*-hydroxy dimethylaniline radical cation could absorb at ~490 nm, and this is the logical intermediate following the triplet oxenium ion given that the stable end product is the reduced *m*-dimethylaminophenol.

4. A ns-TA Experimental Study on the Reactivity of the Triplet *m*-Dimethylamino Phenyloxenium Ion. The results from the ns-TR^3 study on the *m*-dimethylamino phenyloxenium indicated that the triplet *m*-dimethylamino phenyloxenium ion is completely consumed within about 10 μs

DOI: 10.1021/jacs.5b06302
J. Am. Chem. Soc. 2015, 137, 10391−10398

to produce the radical cation in an aqueous solution. The ns-TA experiments show that the band at 356 nm continues to increase in intensity while the band at 494 nm decreases in intensity (see Figure 7). There is an isosbestic point at around

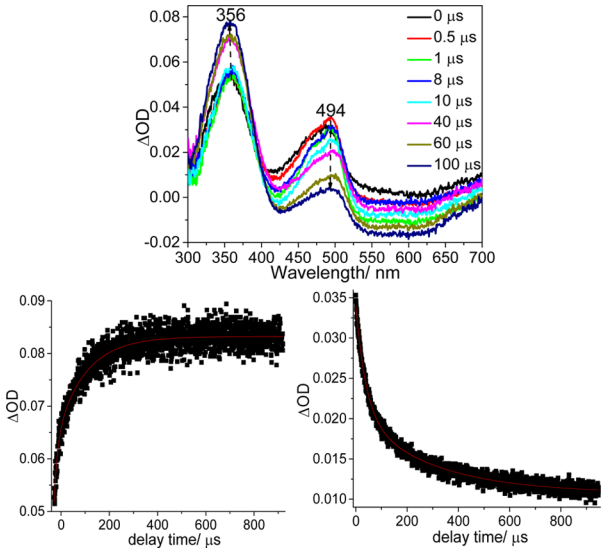

Figure 7. (Top) ns-TA spectra from 0 to 100 μs produced in a MeCN/H_2O 1:1 solution acquired after 266 nm irradiation of the initial precursor compound. See the text for more details. (Bottom) Temporal dependences of the transient absorption intensity of initial compound in a MeCN/H_2O 1:1 mixed solution at 356 nm (left) and 494 nm (right). Solid red line indicates fittings using a biexponential function.

396 nm for this process, indicating a clear transformation between a precursor species and a product species. The temporal dependences of the transient absorption intensity of the initial species in the MeCN/H_2O 1:1 mixed solution with its bands at 356 and 494 nm can be fitted by a biexponential function with two time constants (τ_1 = 1.69 μs, τ_2 = 103 μs) (see Figure 7). According to the ns-TR[3] study, 1.69 μs may be the lifetime of the triplet *m*-dimethylamino phenyloxenium ion and the species having a lifetime of 103 μs is the radical cation. The absorbance that we assign to the *m*-dimethylamino phenol radical cation at 494 nm is also close to the known absorption of the *m*-dimethylaniline radical cation at 470 nm. Putting together all of our observations from the fs-TA, ns-TA, and ns-TR_3 data, we can map out essentially the entire arc of the photochemistry of **1**. These assignments are shown in Scheme 1.

Scheme 1. Proposed Mechanistic Pathway Based on Piecing Together the Spectroscopic Data

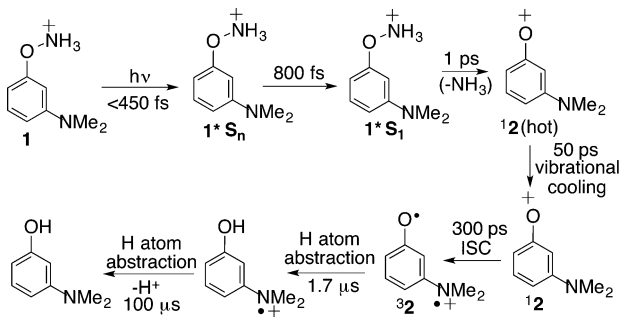

6. Product Studies from Photolysis of 1. Additional evidence for a triplet ground state for the *m*-dimethylamino phenyloxenium ion comes from analysis of the photoproducts. The only detectable photoproduct of **1** in water by ^{1}H NMR is *m*-dimethylaminophenol. This single photoproduct observed from photolysis is in sharp contrast to photolysis of the unsubstituted phenylhydroxylamine hydrochloride, which gave additional nucleophile trapping adducts (e.g., chlorophenol, hydroquinone, catechol, protonated *o*/*p* aminophenols, etc.). In general, one expects nucleophile adducts of a singlet phenyloxenium ion. Reactivity of a triplet phenyloxenium ion is less certain, but by analogy with related reactive intermediates (e.g., carbenes, nitrenes, etc.), one would expect radical ion chemistry (e.g., H atom abstraction). The parent phenyloxenium ion is a singlet ground state ion,[23] so these nucleophile trapping adducts are not surprising. In contrast, the reduced product formed from photolysis of **1** might be expected from a triplet oxenium ion as a result of sequential H atom abstraction processes (followed by loss of a proton) rather than nuclophilic trapping chemistry. Thermolysis studies of **1** led to insoluble tars, likely from oxidation or polymerization (*m*-dimethylaminophenol itself is an electron-rich species and is unstable to oxidation).

7. Cryogenic EPR Studies from Photolysis of 1 in EtOH Glass Indicates Triplet Ground State for 2. Further evidence for the ground state of the *m*-dimethylamino phenyloxenium being a triplet state comes from low-temperature matrix isolation experiments. A low-temperature EtOH glassy matrix photolysis study of **1** (at 4 K), performed in the cavity of an EPR spectrometer, provided the spectrum shown in Figure 8. The signals in the EPR spectrum are consistent with

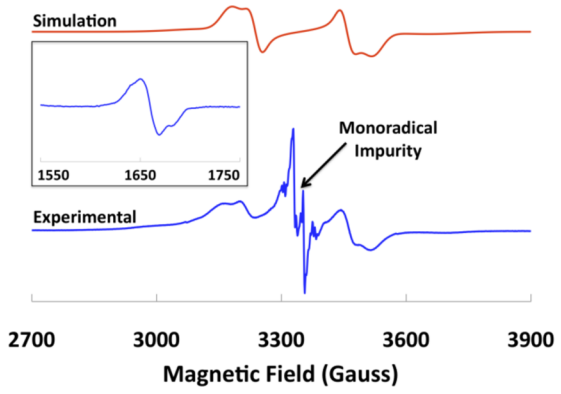

Figure 8. X-band EPR spectrum of **1** irradiated in EtOH glass at 4 K using a mercury lamp source delivered via a fiber optic cable into the cavity. Triplet simulation parameters: D = 280 G ($|D|/hc$ = 0.026 cm^{-1}), $E/|D|$ = 0.075 G (7.0 × 10^{-6} cm^{-1}). Inset: Δm_S = 2 transition.

the formation of a triplet diradical species as well as a monoradical impurity (perhaps arising from a competitive homolysis pathway or from a back electron transfer process). This EPR spectrum provides evidence that the ground state of the oxenium ion is the triplet state, since at 4 K essentially no thermal population of an excited triplet state would be possible outside of having virtually degenerate singlet and triplet energies. The value of the $|D|/hc$ parameter (0.026 cm^{-1}) seen here is very close to that of the *m*-quinone methide $|D|/hc$ parameter (0.027 cm^{-1}) reported by Berson and co-workers,[43] perhaps not surprising given the very similar electronic structure.

DOI: 10.1021/jacs.5b06302
J. Am. Chem. Soc. 2015, 137, 10391−10398

CONCLUSION

In conclusion, using a combination of pulsed laser spectroscopies, we have been able to map out essentially the complete photophysics and photochemistry pathways of **1** in aqueous acetonitrile. This photoprecursor undergoes a photoheterolysis reaction to generate initially the closed-shell singlet oxenium ion and then the triplet oxenium ion after intersystem crossing, which reacts via sequential H atom abstractions to yield a reduced product. One difference between this study and our prior studies with the protonated hydroxylamine photoprecursors is that the photoprecursors for making the phenyloxenium ion and biphenyloxenium ion reported previously gave a mixture of the oxenium ion resulting from a photoheterolysis pathway and the free radical resulting from a photohomolysis pathway of the O−N bond. In this study, we only observe the oxenium ion resulting from the photoheterolysis pathway and do not see transients we can attribute to the free radical. Perhaps the lack of a concomitant homolysis pathway can be attributed to the "meta effect", a term coined by the late Howard Zimmerman[44] to describe the propensity of *meta* pi donors to favor photoheterolysis mechanisms in preference to photohomolysis pathways. This study also permitted the first look at the reactivity of a triplet oxenium ion. In contrast to the singlet state oxenium ions, which react with nucleophiles at the *o*/*p* position on the benzene ring to generate nucleophile-substituted phenols, the triplet state engages in H atom abstractions to yield a reduced product. This triplet reactivity is rather similar to triplet carbenes and triplet nitrenium ions, which can engage in H atom abstraction processes. The π,π^* triplet state of the oxenium ion is longer-lived than the closed-shell singlet state oxenium ions, living for ∼1.7 μs in solution. By comparison, singlet aryloxenium ions have lifetimes of a few nanoseconds in solution. The longer lifetime of the triplet state is similar to carbenes and nitrenes whose triplet states can be seen with nanosecond spectroscopy, while the singlets often have lifetimes on the order of tens of picoseconds.[45] In future work, it would be interesting to compare the reactivity and lifetime of this π,π^* triplet oxenium ion to an n,π^* triplet oxenium ion.

ASSOCIATED CONTENT

Supporting Information

The Supporting Information is available free of charge on the ACS Publications website at DOI: 10.1021/jacs.5b06302.

Synthetic procedures and compound characterization data; product studies; absolute energies and Cartesian coordinates; cryogenic EPR details and simulation parameters (PDF)

AUTHOR INFORMATION

Corresponding Authors

*winter@iastate.edu

*phillips@hku.hk

Notes

The authors declare no competing financial interest.

ACKNOWLEDGMENTS

This work was supported by grants from the Research Grants Council of Hong Kong (HKU 7035/13P) to D.L.P. Partial support from the Grants Committee Areas of Excellence Scheme (AoE/P-03/08) and the Special Equipment Grant (SEG HKU/07) are also gratefully acknowledged. A.H.W. thanks the petroleum research fund, the NSF (1464956), the Cottrell Scholar Award from the Research Corporation for Scientific Advancement, and the ISU chemical instrumentation facility (CIF).

REFERENCES

(1) Vigalok, A.; Rybtchinski, B.; Gozin, Y.; Koblenz, T. S.; Ben-David, Y.; Rozenberg, H.; Milstein, D. *J. Am. Chem. Soc.* **2003**, *125*, 15692.

(2) Swenton, J. S.; Carpenter, K.; Chen, Y.; Kerns, M. L.; Morrow, G. W. *J. Org. Chem.* **1993**, *58*, 3308.

(3) Rieker, A.; Beisswenger, R.; Regier, K. *Tetrahedron* **1991**, *47*, 645.

(4) Rieker, A. *DECHEMA Monogr.* **1992**, *125*, 777.

(5) Pelter, A.; Ward, R. S. *Tetrahedron* **2001**, *57*, 273.

(6) Dimroth, K.; Umbach, W.; Thomas, H. *Chem. Ber.* **1967**, *100*, 132.

(7) Sabot, C.; Guerard, K. C.; Canesi, S. *Chem. Commun.* **2009**, 2941.

(8) Sabot, C.; Commare, B.; Duceppe, M.-A.; Nahi, S.; Guérard, K. C.; Canesi, S. *Synlett* **2008**, *2008*, 3226.

(9) Guérard, K. C.; Chapelle, C. m.; Giroux, M.-A.; Sabot, C.; Beaulieu, M.-A.; Achache, N.; Canesi, S. *Org. Lett.* **2009**, *11*, 4756.

(10) Williams, L. L.; Webster, R. D. *J. Am. Chem. Soc.* **2004**, *126*, 12441.

(11) Peng, H. M.; Webster, R. D. *J. Org. Chem.* **2008**, *73*, 2169.

(12) Taylor, W. I.; Battersby, A. R. *Oxidative coupling of phenols*; Marcel Dekker: New York, 1967; Vol. *1*.

(13) Baesjou, P. J.; Driessen, W. L.; Challa, G.; Reedijk, J. *J. Am. Chem. Soc.* **1997**, *119*, 12590.

(14) Gamez, P.; Gupta, S.; Reedijk, J. *C. R. Chim.* **2007**, *10*, 295.

(15) Osborne, R. L.; Coggins, M. K.; Raner, G. M.; Walla, M.; Dawson, J. H. *Biochemistry* **2009**, *48*, 4231.

(16) Novak, M.; Glover, S. A. *J. Am. Chem. Soc.* **2004**, *126*, 7748.

(17) Wang, Y.-T.; Jin, K. J.; Leopold, S. H.; Wang, J.; Peng, H.-L.; Platz, M. S.; Xue, J.; Phillips, D. L.; Glover, S. A.; Novak, M. *J. Am. Chem. Soc.* **2008**, *130*, 16021.

(18) Winter, A. H.; Falvey, D. E.; Cramer, C. J.; Gherman, B. F. *J. Am. Chem. Soc.* **2007**, *129*, 10113.

(19) Hanway, P. J.; Winter, A. H. *J. Am. Chem. Soc.* **2011**, *133*, 5086.

(20) Hanway, P. J.; Winter, A. H. *J. Phys. Chem. A* **2012**, *116*, 9398.

(21) Katsumata, S.; Lloyd, D. *Chem. Phys. Lett.* **1977**, *45*, 519.

(22) Dewar, M. J. S.; David, D. E. *J. Am. Chem. Soc.* **1980**, *102*, 7387.

(23) Hanway, P. J.; Xue, J.; Bhattacharjee, U.; Milot, M. J.; Ruixue, Z.; Phillips, D. L.; Winter, A. H. *J. Am. Chem. Soc.* **2013**, *135*, 9078.

(24) Xue, J.; Luk, H. L.; Eswaran, S.; Hadad, C. M.; Platz, M. S. *J. Phys. Chem. A* **2012**, *116*, 5325.

(25) Wang, Y.-T.; Wang, J.; Platz, M. S.; Novak, M. *J. Am. Chem. Soc.* **2007**, *129*, 14566.

(26) Li, M.-D.; Hanway, P. J.; Albright, T. R.; Winter, A. H.; Phillips, D. L. *J. Am. Chem. Soc.* **2014**, *136*, 12364.

(27) Li, M.-D.; Ma, J.; Su, T.; Liu, M.; Yu, L.; Phillips, D. L. *J. Phys. Chem. B* **2012**, *116*, 5882.

(28) Li, M. D.; Yeung, C. S.; Guan, X.; Ma, J.; Li, W.; Ma, C.; Phillips, D. L. *Chem. - Eur. J.* **2011**, *17*, 10935.

(29) Runge, E.; Gross, E. *Phys. Rev. Lett.* **1984**, *52*, 997.

(30) O'boyle, N. M.; Tenderholt, A. L.; Langner, K. M. *J. Comput. Chem.* **2008**, *29*, 839.

(31) Merrick, J. P.; Moran, D.; Radom, L. *J. Phys. Chem. A* **2007**, *111*, 11683.

(32) Frisch, M.; et al. *Gaussian09*, revision A.02; Gaussian, Inc.: Wallingford, CT, 2009.

(33) Schmidt, M. W.; Baldridge, K. K.; Boatz, J. A.; Elbert, S. T.; Gordon, M. S.; Jensen, J. H.; Koseki, S.; Matsunaga, N.; Nguyen, K. A.; Su, S.; Windus, T. L.; Dupuis, M.; Montgomery, J. A. *J. Comput. Chem.* **1993**, *14*, 1347.

(34) Lage, M. L.; Fernández, I.; Mancheño, M. J.; Sierra, M. A. *Inorg. Chem.* **2008**, *47*, 5253.

(35) Wang, J.; Kubicki, J.; Peng, H.; Platz, M. S. *J. Am. Chem. Soc.* **2008**, *130*, 6604.

DOI: 10.1021/jacs.5b06302
J. Am. Chem. Soc. 2015, 137, 10391−10398

(36) Webb, S.; Yeh, S. W.; Philips, L. A.; Tolbert, M.; Clark, J. *J. Am. Chem. Soc.* **1984**, *106*, 7286.
(37) Webb, S.; Philips, L. A.; Yeh, S. W.; Tolbert, L. M.; Clark, J. *J. Phys. Chem.* **1986**, *90*, 5154.
(38) Schwartz, B. J.; Peteanu, L. A.; Harris, C. B. *J. Phys. Chem.* **1992**, *96*, 3591.
(39) Toscano, J. P. *Adv. Photochem.* **2001**, *26*, 41.
(40) Du, Y.; Ma, C.; Kwok, W. M.; Xue, J.; Phillips, D. L. *J. Org. Chem.* **2007**, *72*, 7148.
(41) Toscano, J. *Reactive Intermediates Chemistry*; Moss, R., Platz, M., Jones, M., Jr., Eds.; John Wiley and Sons, Inc.: Hoboken, NJ, 2007; p 183.
(42) Chuang, Y. P.; Xue, J.; Du, Y.; Li, M.; An, H.-Y.; Phillips, D. L. *J. Phys. Chem. B* **2009**, *113*, 10530.
(43) Rule, M.; Matlin, A. R.; Hilinski, E. F.; Dougherty, D. A.; Berson, J. A. *J. Am. Chem. Soc.* **1979**, *101*, 5098.
(44) Zimmerman, H. E. *J. Am. Chem. Soc.* **1995**, *117*, 8988.
(45) *Reactive Intermediate Chemistry*; Moss, R. A., Platz, M. S., Jones, M., Eds.; Wiley: New York, 2004.

DOI: 10.1021/jacs.5b06302
J. Am. Chem. Soc. 2015, 137, 10391−10398